J. Electroanal. Chem., 258 (1989) 345–355
Elsevier Sequoia S.A., Lausanne – Printed in The Netherlands

Voltammetric studies and stripping voltammetry of Mn(II) at the wall–jet ring–disc electrode

Christopher M.A. Brett*

Departamento de Química, Universidade de Coimbra, 3049 Coimbra (Portugal)

Maria M.P.M. Neto

Centro de Electroquímica e Cinética da Universidade de Lisboa, Calçada Bento Rocha Cabral 14, 1200 Lisboa (Portugal)

(Received 20 April 1988)

ABSTRACT

The reduction of Mn(II) to manganese amalgam at the mercury thin film wall–jet disc electrode and the oxidation of Mn(II) to MnO_2 at glassy carbon and platinum wall–jet electrodes are investigated. Anodic and cathodic stripping voltammetry with collection of Mn(II) at the wall–jet ring–disc electrode are carried out successfully and compared. Cathodic stripping voltammetry with collection is recommended using glassy carbon electrodes, as these can also be used as substrates for thin mercury film electrodes for metal ions analysed by anodic stripping voltammetry. Optimisation of experimental conditions is discussed.

(I) INTRODUCTION

Manganese is present as a trace element in many biological systems, and as such there is importance in having good methods for determining trace levels of manganese in solution. Fundamental and electroanalytical studies have been undertaken into the reduction and oxidation of Mn(II). Studies into the reduction of Mn(II) are carried out at mercury electrodes to give manganese amalgam [1–3] due to the very negative potential for reduction ($\simeq -1.7$ V vs. SCE). Oxidation to Mn(IV) as the hydrated oxide is done at solid electrodes — glassy carbon or platinum [4,5]. The determination of trace levels has been achieved by anodic stripping voltammetry (ASV) [6,7], cathodic stripping voltammetry (CSV) [4,5,8–10], or by adsorptive stripping voltammetry [11].

* To whom correspondence should be addressed.

0022-0728/89/$03.50

We have been investigating stripping voltammetry with collection (SVWC) [12] at the wall–jet ring–disc electrode (WJRDE) [13] and in this work compare anodic and cathodic SVWC of manganese(II) and look at various aspects of the electrode reactions. In the former case we used a mercury thin film electrode deposited in situ on a glassy carbon substrate, and in the latter glassy carbon and platinum electrodes. One of the advantages of using glassy carbon is that we can perform reductions or oxidations at the same electrode without needing to change electrodes - - we simply change the solution flowing past the electrode and the applied potential. The importance of the wall–jet electrode is due to its hydrodynamic characteristics [13,14] and its use as a versatile on-line detector. In many applications this could include the determination of manganese, as would be the case for nutrient solutions for hydroponic cultures [15].

(II) THEORETICAL BASIS

In the stripping voltammetry with collection technique at double hydrodynamic electrodes [12] a species deposited at an electrode during time t_{dep} is stripped by a step change in potential and collected at a downstream electrode whose potential remains constant at the deposition potential for the species during the entire operation. The resulting current transient will be almost entirely free of non-Faradaic contributions. Although the shape of the transient will depend on the type of fluid flow, its integral will not [16]. The relationship obtained, exemplified for a wall–jet ring–disc electrode, is

$$q_R = -N_0 i_{D,L} t_{dep} \tag{1}$$

where q_R is the charge under the ring current transient peak, t_{dep} the deposition time at the disc electrode, N_0 the steady state collection efficiency, and $i_{D,L}$ the disc diffusion-limited current [13] during deposition given by

$$i_{D,L} = 1.38nFD^{2/3}\nu^{-5/12}a^{-1/2}V_f^{3/4}r_1^{3/4}c_\infty \tag{2}$$

where V_f is the volume flow rate, a the jet (nozzle) diameter, r_1 the disc electrode radius, and all other symbols have their usual meaning. After we have determined or measured values of the various parameters we obtain a relationship of the form

$$c_\infty = \text{const.}(q_R/t_{dep}) \tag{3}$$

By use of the standard addition method we can compare concentrations calculated from eqn. (3) with the quantity added.

(III) EXPERIMENTAL

The construction of the wall–jet ring–disc electrode assembly and cell have been described previously [16]; the cell contains a platinum tube auxiliary electrode, also serving as solution outlet, and an Ag/AgCl reference electrode; the nozzle/ring–disc electrode separation was 3 mm throughout to ensure wall–jet behaviour. Ring–disc

electrodes were constructed with glassy carbon disc and platinum ring, or disc and ring both of glassy carbon — designated GC–Pt and GC–GC respectively. Electrode radii were $r_1 = 1.591$, $r_2 = 1.724$, $r_3 = 1.898$ mm (GC–Pt electrode) and $r_1 = 1.613$, $r_2 = 1.743$, $r_3 = 1.998$ mm (GC–GC electrode), where r_1 is the disc radius, r_2 is the inner radius of the ring and r_3 is its outer radius. This leads to theoretical collection efficiencies of 0.141 and 0.174. Experimental collection efficiencies, which were invariant with flow rate, were 0.163 ± 0.002 and 0.183 ± 0.002 respectively. The higher experimental values reflect the finite volume of the wall–jet cell, but were entirely reproducible. In the application of eqn. (3) we use the experimental values. Kinematic viscosities were measured with an Ostwald viscometer and diffusion coefficients using submillimolar concentrations of Mn(II), measuring $i_{D,L}$ and calculating from eqn. (2).

Solution was sucked through the wall–jet cell by a peristaltic pump (Pharmacia P-3), having been previously deoxygenated by bubbling oxy-free nitrogen (Ar Líquido, Grade U) for 15 min before the experiments and during their execution.

An Oxford Electrodes bipotentiostat was used to control potentials, modified to include a bounce-free switch in order to switch from deposition to stripping potentials at the disc electrode and an integrator to integrate the ring current. Integrated transients were registered on a Philips PM8143 X–Y–t recorder.

Solutions were all prepared from Merck pro analysi reagents or equivalent using water distilled from permanganate and then distilled twice further. Standard additions of Mn(II) were made from stock solutions of 10^{-3} *M* or 10^{-4} *M* $MnSO_4$. A stock solution of 10^{-2} *M* Hg(II) was prepared from $Hg(NO_3)_2$ by dissolution in HNO_3 at pH 2 and kept in the dark; this was added to the electrolyte solution such that the concentration of Hg(II) was 5×10^{-5} *M* in the plating solutions.

(IV) RESULTS AND DISCUSSION

(IV.1) Reduction of Mn(II) to Mn(Hg)

(IV.1.i) Linear sweep voltammetry

The potential necessary to reduce Mn(II) to Mn(Hg) is very negative and so use of a mercury electrode is unavoidable. We co-deposited a thin mercury film with the manganese ions on a glassy carbon substrate at -1.75 V vs. Ag/AgCl in order to ensure limiting current deposition. The dc scan (5 mV s^{-1}) in Fig. 1 shows that the metal is stripped in a quasi-reversible process since the peak width at half-height $b_{1/2} \simeq 60$ mV as opposed to $b_{1/2} = 37.5$ mV for a reversible 2 e^- process [17]. Previous studies of the reduction of Mn(II) to Mn(Hg) have also shown that the electrode kinetics is not as fast as for some other heavy metals such as Cu [1,2]. With respect to the supporting electrolyte best wave definition and narrowest peak (fastest redissolution kinetics) were found with sodium perchlorate; a kinetic study at the DME reached the same conclusion [3].

The second dc scan of Fig. 1 was obtained at a scan rate of 100 mV s^{-1}. Here we see a further wave appearing at more positive potentials and the wave shape reflects

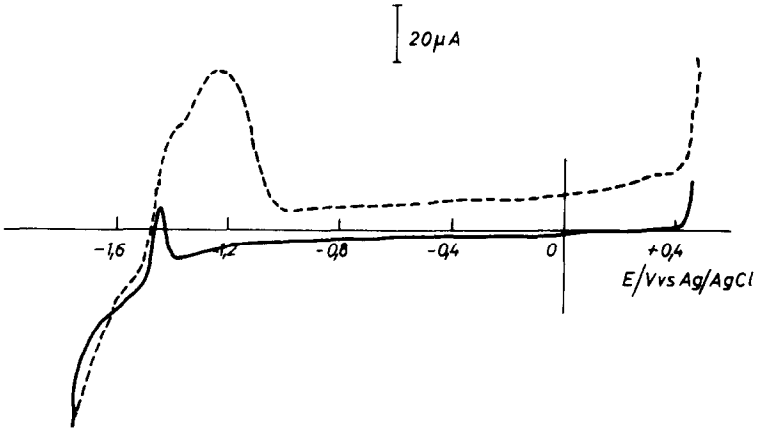

Fig. 1. Linear sweep voltammogram for the redissolution of manganese at the wall-jet mercury thin film disc electrode, formed on GC substrate. Deposition time 60 s at -1.75 V. Solution: 10^{-5} M Mn^{2+}, 5×10^{-5} M Hg(II), 0.1 M $NaClO_4$. $V_f = 0.034$ cm^3 s^{-1}. Scan rate = 5 mV s^{-1} (———), 100 mV s^{-1} (- - - - -).

the non-reversible nature of the electrode process. This shows that dc ASV is not suited to the determination of Mn(II); ASVWC should be a significant improvement.

(IV.1.ii) ASVWC

The standard addition method was used to construct calibration curves. The expression obtained for the relation between q_R/t_{dep} and c_∞ is, analogously to eqn. (3)

$$c_\infty = -96.1 \left(q_R/t_{dep}\right) \text{ mol cm}^{-3} \tag{4}$$

where $\nu = 0.895 \times 10^{-2}$ cm^2 s^{-1} and $D = 6.4 \times 10^{-6}$ cm^2 s^{-1}. The ring potential, E_R, was kept constant at -1.75 V vs. Ag/AgCl during the whole of the experiment; after each experiment the disc electrode was stripped of the mercury film at $+0.5$ V — this procedure was found to give the best results. Figure 2 shows a typical set of calibration curves and Fig. 3 a comparison of added Mn(II) vs. that theoretically predicted from eqn. (4) — as can be seen, the relation between the two is described by a line of slope $\simeq 0.5$ whereas it should be of unity. The fact that the line slope is 0.5 would suggest, at first sight, the possibility of a 1 e^- oxidation. This is extremely unlikely, and we believe that the value of the slope is fortuitous in this sense.

The lack of agreement between experiment and theory may be explained by two factors. Firstly, the deposition occurs at a very negative potential and close to hydrogen evolution (see Fig. 1). Secondly, the solubility of manganese in mercury is very low (0.0006 atom%) [18]. Both these factors would result in a decrease in the amount of manganese(II) reduced to form the amalgam.

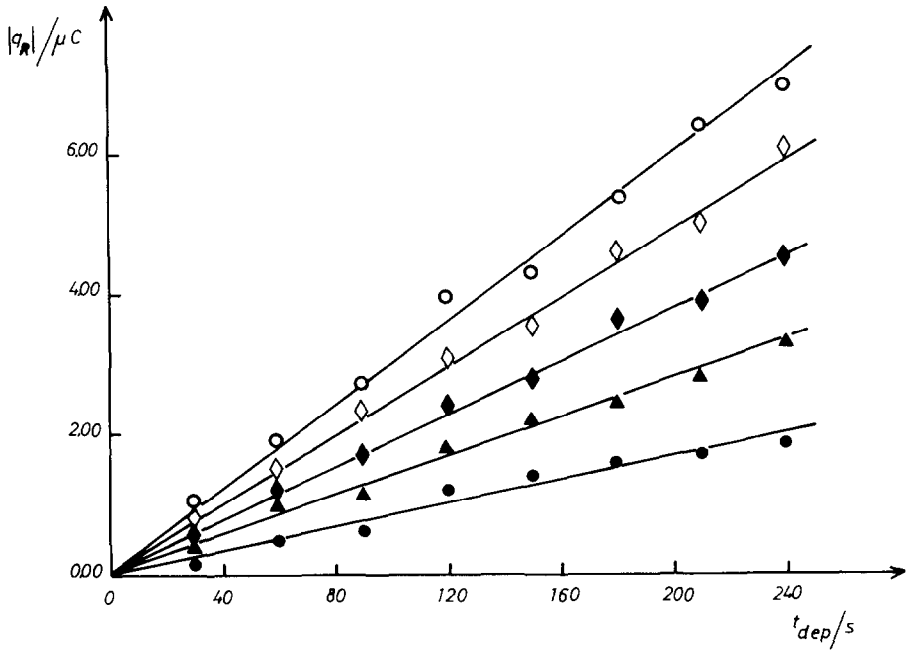

Fig. 2. ASVWC at GC–GC WJRDE showing successive additions of 10^{-6} M Mn^{2+}. Experimental conditions as in Fig. 1. $E_{D,dep} = -1.75$ V; $E_{D,strip} = -1.35$ V; $E_R = -1.75$ V vs. Ag/AgCl. [Mn(II)] added/μmol dm^{-3}; (○) 5.0; (◇) 4.0; (◆) 3.0; (▲) 2.0; (●) 1.0.

There is evidence that at high manganese concentrations, when the concentration is approaching saturation, there is formation of Mn_2Hg_5 as a dispersed phase, which cannot be reoxidised [2]. However, at the manganese levels studied here we can assume that this is not occurring as it would lead to a levelling off in the

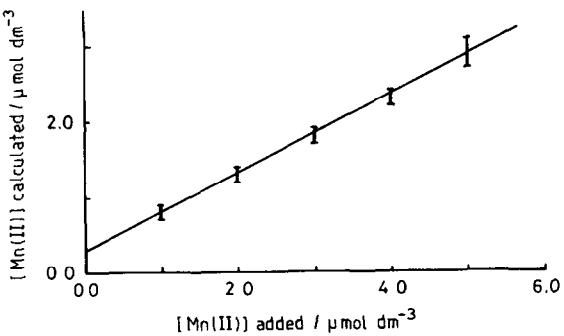

Fig. 3. Plot of Mn(II) concentrations calculated from eqn. (4) vs. Mn(II) added. Data from Fig. 2. Line has slope –0.5.

response. Additionally, since the mercury is co-deposited with the manganese the concentration within the mercury film should be constant and independent of radial position; for a pre-plated mercury film this would not necessarily be the case.

Nevertheless, the results obtained show good reproducibility, and so by working from calibration curves we can use the technique.

(IV.1.iii) Interference and matrix effects in ASVWC

We also investigated the effect of interferences from other heavy metals which can be co-deposited from aqueous solution and incorporated into the amalgam. Formation of a copper + manganese intermetallic compound has already been described [7], resulting in a 50% depression of the Mn peak when the concentration of Cu is ten times that of Mn. In most real-life situations, there is usually much more Mn than Cu; also, when there is Cu there is also Zn and preferential formation of the Cu + Zn intermetallic compound. By judicious choice of the experimental conditions, even when there is interference between two elements they can be resolved by subtractive techniques [15], or by addition of a third element [7]. At the wall–jet mercury thin film electrode we found no interference problem from Cu in the determination of Mn when [Mn(II)] = 2[Cu(II)] = 2[Zn(II)].

(IV.2) Oxidation of Mn(II) to MnO_2

Hydrated manganese dioxide is formed by the anodic oxidation of solutions containing Mn(II), the potential for deposition being a function of solution pH [19], as predicted from the generic half-reaction

$$Mn^{2+}(H_2O)_x \rightarrow MnO_2(H_2O)_{x-y}(s) + 4\,H^+ + (y-2)\,H_2O + 2\,e^-$$

and of the electrode material. A comparison between platinum and glassy carbon electrodes and electrolyte buffer solutions was made, followed by an evaluation of cathodic stripping voltammetry with collection.

(IV.2.i) Platinum vs. glassy carbon electrodes

In Fig. 4 are shown voltammograms obtained for platinum and glassy carbon wall–jet disc electrodes using borate buffer supporting electrolyte at pH 7.2. Both electrode materials give rise to two reduction peaks, those at platinum being slightly narrower than at glassy carbon and at more positive potential, a manifestation of faster MnO_2 dissolution electrode kinetics. The more positive peak at the GC electrode is barely visible. However, for the purpose of cathodic stripping voltammetry the two electrode materials should be equally good. The existence of two reduction peaks will be discussed below.

(IV.2.ii) Buffer and pH considerations

As stated above, the solution pH affects the potential necessary for the formation of the MnO_2 deposit, and also its removal. Thermodynamic considerations lead us to predict a variation in reduction peak position of 118 mV more negative for each

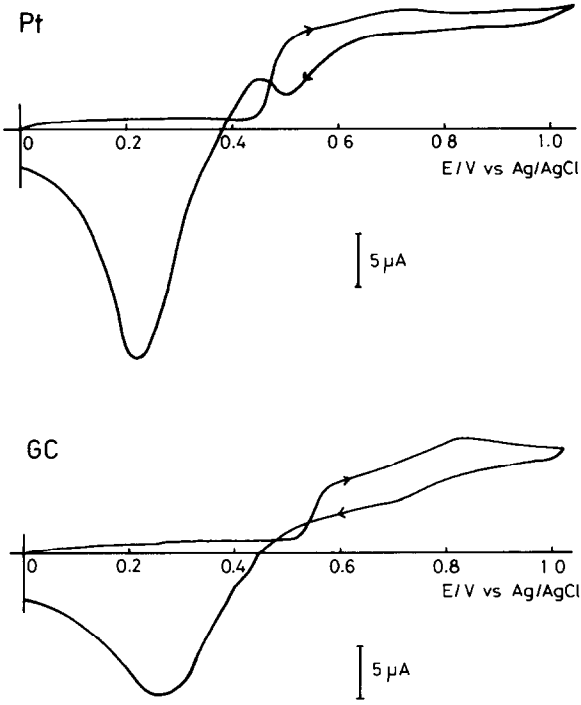

Fig. 4. Cyclic voltammograms of Mn(II) at Pt and GC wall-jet disc electrodes in 0.2 *M* borate buffer + 0.1 *M* KCl at pH 7.2. [Mn(II)] = 10^{-4} mol dm^{-3}. $V_f = 0.040$ cm^3 s^{-1}. Scan rate 5 mV s^{-1}.

unit increase in pH, which will be followed for a reversible reduction redissolution process.

At low pH there is a tendency for incomplete precipitation of the insoluble dioxide; at high pH a tendency for $Mn(OH)_2$ to precipitate — the extent to which this will affect the electrode reaction depends on the solubility product ($K_s = 2 \times 10^{-13}$). For these reasons it is advisable to use a buffer electrolyte in neutral or slightly acidic solution.

We looked at both phthalate and borate buffers, phosphate being impossible because of the precipitation of $Mn_3(PO_4)_2$. Figure 5 shows cyclic voltammograms obtained in phthalate buffer at GC, which should be considered together with those in Fig. 4 for borate buffer. Phthalate gives the best response, i.e. the narrowest stripping peak, in the region between pH 5 and pH 5.9 and borate at around pH 7, the latter in accordance with previous findings [9]. The change in peak position for phthalate buffer with pH is significantly more than 118 mV per pH unit, being closer to this value for borate, once again reflecting the electrode kinetics. For this reason we preferred to use borate buffer.

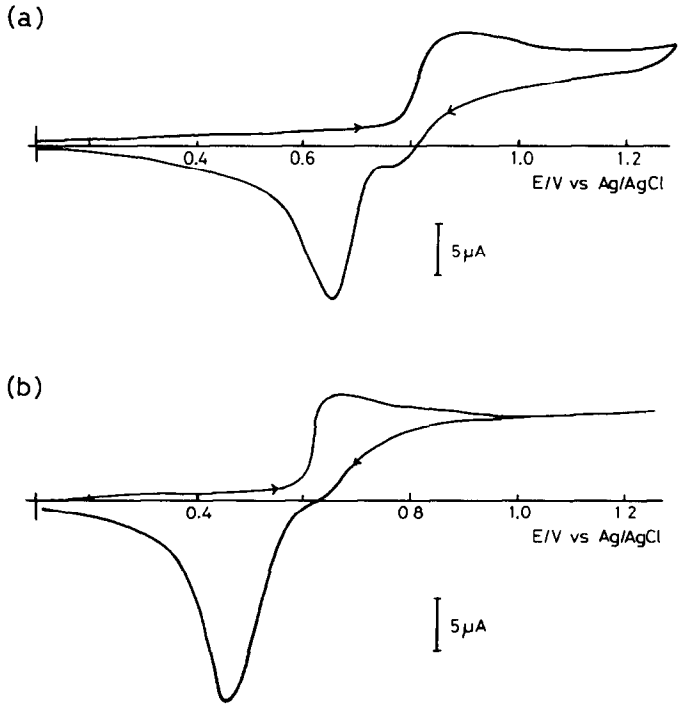

Fig. 5. Cyclic voltammograms of Mn(II) at the GC wall-jet disc electrode in 0.2 *M* phthalate buffer at (a) pH 5.1. (b) pH 5.9. Other experimental conditions as in Fig. 4.

(IV.2.iii) The nature of the MnO_2 deposit

There are, in fact, two stripping peaks of MnO_2, evident in Figs. 4 and 5, a small peak at a potential coinciding approximately with that necessary for the formation of the MnO_2 deposit and a much larger one at more negative potential. The existence of two peaks has already been noted [5,9]. Various explanations have been offered for the presence of the first, more positive, reduction peak:

(i) Reduction of Mn(IV) to Mn(III) — probably as MnOOH [9].

(ii) Two different types of MnO_2 layer are formed with different reduction potentials [9].

(iii) Reduction of excess non-stoichiometric oxygen in the manganese dioxide layer (based on a rotating ring–disc electrode study which showed no ring current corresponding to soluble products of the more positive reduction peak, implying that the product is non-electroactive) [5].

Our CSVWC results, see below, imply that the manganese dioxide is essentially stoichiometric. Maskell and co-workers [20,21] studied the reduction of MnO_2 formed in acidic solutions, and found evidence for the formation of a deposit in two types of layer, where there is more than a monolayer deposit, corresponding to the surface region of crystallites in contact with the solution and to their interior, each

with different conducting properties. This suggests an explanation involving two layers as being reasonable. The first reduction peak could correspond to reduction to an insoluble form of Mn(III) at the surface layers in contact with the solution (near the middle of the disc electrode where we will have multilayer deposition) without any liberation of free Mn^{3+}. In this way all the experimental evidence can be satisfied, especially when we take into account the fact that the more positive reduction peak becomes proportionally smaller with respect to the more negative peak as we reduce the Mn(II) concentration or the deposition time.

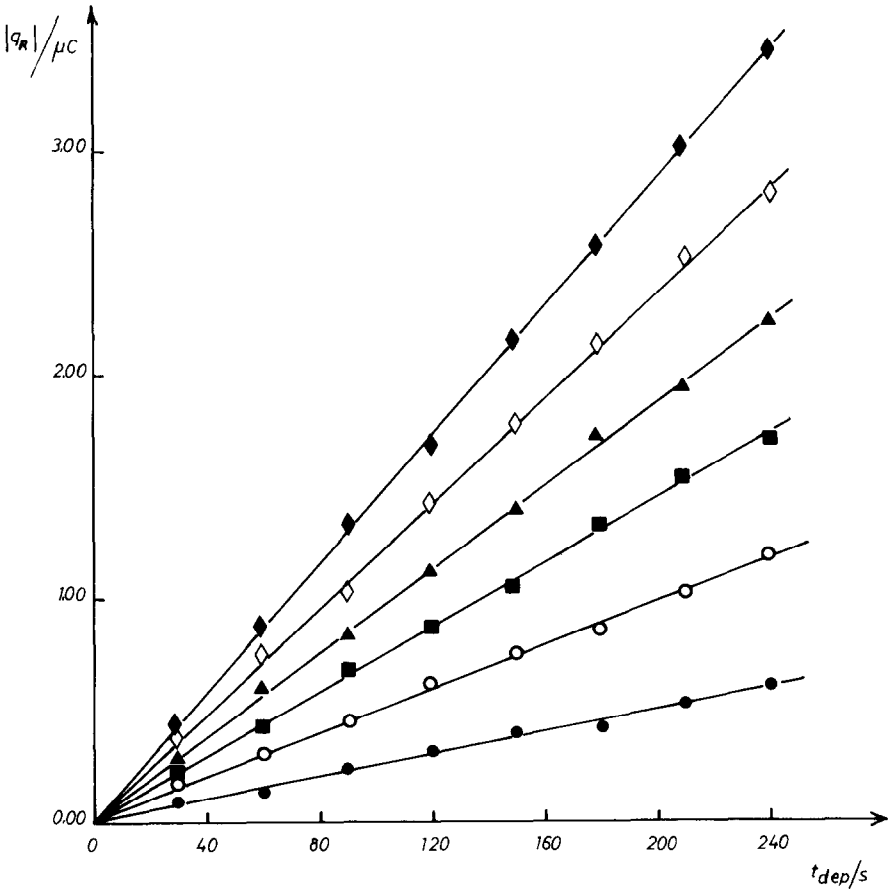

Fig. 6. CSVWC at GC–GC WJRDE showing successive addition of 0.2×10^{-6} M Mn^{2+}. Electrolyte: 0.2 M borate buffer + 0.1 M KCl at pH 7.2. $V_f = 0.032$ cm^3 s^{-1}. $E_{D,dep} = +0.75$ V; $E_{D,strip} = 0.0$ V; $E_R = +0.75$ V vs. Ag/AgCl. [Mn(II)] added/μmol dm^{-3}: (◆) 1.2; (◇) 1.0; (▲) 0.8; (■) 0.6; (○) 0.4; (●) 0.2.

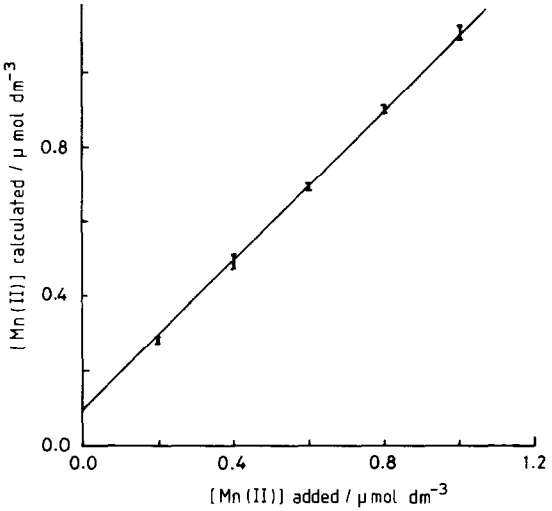

Fig. 7. Plot of Mn(II) concentrations calculated from eqn. (6) vs. Mn(II) added. Data from Fig. 6. Line has unity slope.

(IV.2.iv) CSVWC

The relationships analogous to eqn. (3) are in this case

$$\text{GC–Pt WJRDE:} \quad c_\infty = 81.7\left(q_R/t_{dep}\right) \text{ mol dm}^{-3} \tag{5}$$

$$\text{GC–GC WJRDE:} \quad c_\infty = 89.4\left(q_R/t_{dep}\right) \text{ mol dm}^{-3} \tag{6}$$

where $\nu = 0.891 \times 10^{-2}$ cm^2 s^{-1} and $D = 7.3 \times 10^{-6}$ cm^2 s^{-1}. Typical results of the CSVWC experiments are illustrated in Figs. 6 and 7 for the GC–GC WJRDE using the method of standard addition. The intercept in Fig. 7 corresponds to the blank value, and the line drawn has unity slope. Good reproducibility and accuracy are obtained for both electrodes. It is thus easier to detect low concentrations of Mn(II) by CSVWC than by ASVWC. We recommend preferential use of a GC–GC electrode, since it can also be used as substrate for mercury thin film electrodes.

(V) CONCLUSIONS

Voltammetric studies of the reduction and oxidation of Mn(II) lead to the parameters necessary for its electroanalytical determination. Comparison of the methods of anodic and cathodic stripping voltammetry with collection at the wall–jet ring–disc electrode has shown that both can be used for the reliable determination of manganese, the former giving signals approximately half that predicted by theory. For this reason, cathodic stripping voltammetry is to be preferred.

Analysis of linear scan voltammetric stripping curves and the CSVWC results for manganese dioxide show that the electrodeposit is essentially stoichiometric and

that the double reduction peak obtained probably results from the presence of two different types of oxide layer on the substrate.

Glassy carbon is the preferred electrode material, as it permits good CSVWC results, as well as being a good and effective substrate for thin mercury films in ASV studies of other heavy metal ions present. Thus the same flow-through cell can be used for various determinations without it being necessary to change electrodes.

REFERENCES

1 J. Biernat and J. Koryta, Collect. Czech. Chem. Commun., 25 (1960) 38.
2 A. Dowgird and Z. Galus, J. Electroanal. Chem., 34 (1972) 457.
3 S.S. Sharma and M. Singh, J. Indian Chem. Soc., 57 (1980) 21.
4 Kh.Z. Brainina, Zh. Anal. Khim., 19 (1964) 810.
5 E. Kostihová and P. Beran, Collect. Czech. Chem. Commun., 47 (1982) 1216.
6 R.J. O'Halloran and H. Blutstein, J. Electroanal. Chem., 125 (1981) 261.
7 R.J. O'Halloran, Anal. Chim. Acta, 140 (1982) 51.
8 C.O. Huber and L. Lemmert, Anal. Chem., 38 (1966) 128.
9 E. Hrabánkova, J. Dolezal and V. Masin, J. Electroanal. Chem., 22 (1969) 195.
10 A. Trojánek and F. Opekar, Anal. Chim. Acta, 126 (1981) 15.
11 J. Wang and J.S. Mahmoud, Anal. Chim. Acta, 182 (1986) 147.
12 D.C. Johnson and R.E. Allen, Talanta, 20 (1973) 305.
13 W.J. Albery and C.M.A. Brett, J. Electroanal. Chem., 148 (1983) 201.
14 C.M.A. Brett and A.M. Oliveira Brett in C.H. Bamford and R.G. Compton (Eds.), Comprehensive Chemical Kinetics, Vol. 26, Elsevier, Amsterdam, 1986, Ch. 5.
15 C.M.A. Brett and M.M.P.M. Neto, J. Chem. Soc. Faraday Trans. 1, 82 (1986) 1071.
16 W.J. Albery and C.M.A. Brett, J. Electroanal. Chem., 148 (1983) 211.
17 W.T. de Vries and E. van Dalen, J. Electroanal. Chem., 14 (1967) 315.
18 M.T. Kozlovskii, A.I. Zebreva and V.P. Gladyshev, Amalgamy i ikh Primenenie, Izd. Nauka, Alma-Ata, 1971.
19 Kh.Z. Brainina and N.K. Kiva, Zh. Anal. Khim., 22 (1967) 536.
20 W.C. Maskell, J. Electroanal. Chem., 198 (1985) 127.
21 J.A. Lee, W.C. Maskell and F.L. Tye, J. Electroanal. Chem., 79 (1977) 79.